Engineering Analysis with Boundary Elements 34 (2010) 492–500

Contents lists available at ScienceDirect

Engineering Analysis with Boundary Elements

journal homepage: www.elsevier.com/locate/enganabound

Misfit functional for recovering data in 2D ElectroCardioGraphy problems

N. Hariga-Tlatli [a,*], T.N. Baranger [b], J. Erhel [c]

[a] LAMSIN-ENIT & INAT, Tunisia
[b] Université de Lyon, CNRS, Université Lyon 1, INSA-Lyon, LaMCoS UMR5259, F-69621 Villeurbanne, France
[c] INRIA, Campus de Beaulieu, 35042 Rennes, France

ARTICLE INFO

Article history:
Received 9 April 2009
Accepted 22 December 2009

Keywords:
ElectroCardioGraphy
Noninvasive method
Data completion
Inverse problem
Cauchy problem
Generalized least-squares

ABSTRACT

This paper focuses on the inverse ElectroCardioGraphy problem which consists in recovering the electrical potential and flux on the heart from electrical potential on the body surface. An energy-like error functional introduced in Andrieux et al. [3] and a generalized least-squares method are performed in the context of this ill-posed problem of missing boundary data recovering. Numerical experiments with 2D domains highlight the efficiency of the proposed methods as well as their robustness in the model context.

© 2010 Elsevier Ltd. All rights reserved.

1. Introduction

The aim of this paper is to solve the inverse ElectroCardioGraphy (ECG) problem by means of an energy-like error functional and a generalized least-squares method.

The general framework of our contribution consists in recovering lacking data on some part of the boundary of a domain from overspecified data on the remaining part of the boundary. This kind of problem occurs in the reconstruction of cardiac activity. In fact, noninvasive imaging of heart's electrical activity from ElectroCardioGram becomes a standard diagnosis tool in clinical application. The reconstruction of the spread of electrical excitation in the human heart of each single beat shall facilitate cardiologists to discriminate normal from abnormal activity, localize the origin of arrhythmias, ischemie or infarcted regions [25]. Thus, the aim of the inverse problem in ElectroCardioGraphy is to recover noninvasively regional information about intracardiac electrical events from electrical measurements on the body surface. For this scope there are two classes of formulations based on different *equivalent representations* of the intra-cardiac sources: formulation in terms of activation wavefronts or potential distributions [22].

The first type is based on the fact that during the spread of activation in the heart, the most significant bioelectric source is the large potential difference that exists across the moving wavefront dividing active tissue from resting one. Therefore, researchers have developed source representations leading to tractable inverse problem directly modeling this wavefront [19]. However, the disadvantage of this method is that it covers only the activation wavefronts and does not give information about repolarization or recovery. In addition, it does not reflect the effects of anisotropic conduction. In fine it requires to do a surgery for putting the electrodes in the heart tissue.

The second type of formulation represents the intra-cardiac sources in terms of the distribution of the electrical potential on a closed surface that completely separates the sources from the observations. The field anywhere on the observation side of such a surface has a one-to-one association with the potential distribution on the surface itself. Thus the potential distribution on this surface represents an equivalent source. One such ideal surface is the epicardium, the outer surface of the heart, with measurements made on the body surface. A second variant of the potential distribution formulation takes the inner surface of the heart, the endocardium, as the bounding surface representing the source, see Khoury et al. [21]. But in this case an intracavitary probe is introduced surgically.

One strength of the potential based formulations is that they are more general, they recover the potential anywhere on the surface or within the appropriate volume conductor at any point in the cardiac cycle. Furthermore they can take account of the heterogeneity of the body.

Both of the methods described above share certain common assumptions: quasi-static propagation, temporally constant geometry, a torso with conductivity, a linear medium, potentials recorded with respect to a common reference and insignificant noncardiac electrical activity. Given these assumptions many

* Corresponding author.
E-mail addresses: tlatli.nejla@inat.agrinet.tn (N. Hariga-Tlatli), thouraya.baranger@univ-lyon1.fr (T.N. Baranger), jocelyne.erhel@inria.fr (J. Erhel).

0955-7997/$ - see front matter © 2010 Elsevier Ltd. All rights reserved.
doi:10.1016/j.enganabound.2009.12.006

numerical methods were developed for solving the forward and the inverse problem. However, the boundary element method (BEM) and the finite element method (FEM) remain the main numerical approaches. The final result of all these approaches is a simple description of the relationship between sources and remote body-surface or probe-surface potentials. For the epicardial to body surface formulation, for example, we have $u_T = \mathcal{T} u_H$, with u_T and u_H the body surface and the epicardial potentials, respectively, and $\mathcal{T}$ is a transfer function weighting the contribution of each epicardial site to the potential at each body surface site.

However, the formulation of a useful inverse model does not follow directly from the source models and forward solutions described above, because of the ill-posed nature of the inverse problem, the ambiguities of various source models, the error in any forward solution and the presence of noise in measured data. So we need to find a way to select the best solution from the available information. The most straightforward way is to look for the solution that minimizes the difference between the torso measurements predicted by a certain solution together with the forward model, on one hand, and the actual measured data on the other hand. This difference, the residual error, is measured in terms of L_2 norm in the least-squares method. But the effect of the ill-posedness character of the inverse problem is that solutions will be unreliable and often unrealistic. Consequently we have to regularize the solution by minimizing a weighted sum of two terms: one term is the residual error and the other is a penalty term describing an undesirable property of the solution as shown by MacLeod et al. [22].

In the classical regularized least-squares approach, the transfer function $\mathcal{T}$ is used to define the residual error [15]. Here we introduce a generalized regularized least-squares approach, where the body surface potential is related to both the epicardial potential and current. We also define another approach, based on an energy misfit functional. A common feature is that both methods recover simultaneously the epicardial potential and current.

The paper is organized as follows:

- Section 2 is devoted to the description of the mathematical model.
- In Section 3 the modeling Cauchy problem for Laplace's equation is described.
- In Section 4 we define, in the continuous framework, two misfit functionals namely, an energy like error functional and a generalized least-squares one.
- In Section 5 we present the discretized form of the two previous functionals.
- Section 6 deals with numerical experiments on 2D domains and some comments.
- The paper ends with some concluding remarks.

2. The mathematical model

A general volume conductor can be defined as a region of volume Ω, with a conductivity σ, in which resides a source current I_V per unit volume. Solving a volume conductor problem means finding expressions for the electric **E** and potential **u** fields everywhere within the domain Ω.

The bioelectric current sources I_V, rise from excitable cells undergoing an activation process. The cardiac activation gives arise to such current. As I_V is, in general, time-varying the resulting field quantities are governed by Maxwell's equations. For the macroscopic volume conductor problem, in which we do not consider the individual membrane currents, we can use a quasi-static approximation [20].

In Table 1 we show the conductivity σ and relative permittivity ε_R values for some tissues. The permittivity ε which is the product of the permittivity of free space $\varepsilon_0 = 8.85 \times 10^{-12}$ (F/m) by the relative permittivity ε_R, is very small. Thus the displacement current is much smaller than the conduction current. Consequently Maxwell's equations are reduced to a Poisson's one. The general form of Poisson's equation for electrical conduction is

$$\nabla \cdot \sigma \nabla u = -I_V \quad \text{in } \Omega. \tag{1}$$

In this form, one includes the source region and an understanding of the primary bioelectric sources, I_V. Alternatively, one can define a surface bounding the region which includes the sources. The formulation in terms of information on that surface yields to Laplace's equation:

$$\nabla \cdot \sigma \nabla u = 0 \quad \text{in } \Omega. \tag{2}$$

Estimating the cardiac potential distribution from the body-surface potential is referred to as *inverse problem of ElectroCardio-Graphy*. In this paper we formulate the inverse problem of ECG in terms of epicardial potentials and thus to use Laplace's equation. Therefore the ECG problem is rephrased as follows: Let Ω be the volume of the thorax, Γ_T the surface of the torso, Γ_H the surface of the heart such that they constitute a partition of the whole boundary $\partial\Omega$ and n the unitary normal vector on the boundary. Given a zero current density since the air around the body is insulating, and the corresponding potential T on the torso surface, one wants to recover the corresponding flux and potential on the heart surface. The most general setting takes into account both the non inhomogeneities and the anisotropy, in that case the conductivity is a variable matrix [22]. The model problem is

$$\begin{cases} \nabla \cdot \sigma \nabla u = 0 & \text{in } \Omega, \\ \sigma \nabla u \cdot n = 0 & \text{on } \Gamma_T, \\ u = T & \text{on } \Gamma_T. \end{cases} \tag{3}$$

This problem is known since Hadamard to be illposed in the sense that the dependence of u on the data T is not continuous [16]. We propose, in this paper, to reconstruct the lacking data using an energy-error functional introduced in Andrieux et al. [3] and the generalized least-squares method regularized by the Tikhonov procedure studied by Erhel et al. [11] and Hechme [18].

3. Data completion

Let us consider the above Cauchy problem (3). Provided the data T is compatible with a null flux, which means that the pair $(T,0)$ is indeed the trace and normal trace of a unique harmonic function u, extending the data means finding (φ, t) such that

$$\begin{cases} \nabla \cdot \sigma \nabla u = 0 & \text{in } \Omega, \\ u = T,\ \sigma \nabla u \cdot n = 0 & \text{on } \Gamma_T, \\ u = t,\ \sigma \nabla u \cdot n = \varphi & \text{on } \Gamma_H. \end{cases} \tag{4}$$

The question is how to reconstruct numerically the pair (φ, t). In practical problems data are not expected to be compatible, since data errors may occur by measurements errors as well as discretization ones. The ill-posedness in Hadamard's sense shows up—dramatically—when one tries to approximate the given data T: it is possible to approach it as closely as desired on Γ_T by traces

Table 1
Conductivity and relative permittivity of some human tissues [23].

Tissue type	Conductivity (S/m)	Relative permittivity
Aorta	0.478	56.01
Heart	0.765	84.30
Lungs	0.315	29.48
Bone	0.067	14.72

of a single harmonic function, the *surprise* being a hectic behavior of this function on the remaining part of the boundary. Regularization procedures are therefore required to treat the data completion problem. There are several approaches to regularize such ill-posedness. Some of them transform the ill-posed problem into a well-posed one by adding a penalty term or by mollifying the data in order to avoid data oscillations. Tikhonov like methods use the penalty approach [29]. The classical least-squares procedure encountered in the literature, for example Cimetiére et al. [9], recovers the Dirichlet condition and estimate the Neumann one in a post-processing step, consequently the Neumann data is not identified accurately. We define a new approach, still using Tikhonov method, but with generalized least-squares. This new method recovers both Dirichlet and Neumann conditions. However, this approach needs to estimate a regularization parameter [11,18]. We use also an another method [3], which is based on an energy like misfit function. In this method, we introduce two distinct fields each of them meeting only one of the overspecified data. Moreover, with this method, there is no need to add a penalty term and thus there is no parameter to tune.

4. Misfit functionals

We resort in this work to two misfit functionals of least-squares type. The first one is a measurements to computations misfit function and the second one is built on the energy norm. Observe that, when the complete data are available on Γ, we have an overspecified boundary value problem described by Eqs. (4).

4.1. The classical and generalized least-squares functionals

In this part, we consider a 2D domain Ω and a homogeneous conductivity σ. The method could be extended to 3D domains. Let us consider the measurements to computations misfit function:

$$\min \|u-T\|_{L^2(\Gamma_T)}, \tag{5}$$

where u is the solution of the following wellposed mixed value problem:

$$\begin{cases} \nabla\cdot\sigma\nabla u=0 & \text{in } \Omega,\\ u=\tau & \text{on } \Gamma_H,\\ \sigma\nabla u\cdot n=0 & \text{on } \Gamma_T. \end{cases} \tag{6}$$

Notice that this least-squares formulation has been studied in Chakib et al. [7] resorting to the optimal control tools.

We resort to the boundary integral representation of the forward problem, where the heart potential and the flux are simultaneously considered:

$$u(x)=\int_{\partial\Omega}\left(\frac{\partial u(y)}{\partial n}\mathcal{U}(x,y)-u(y)\frac{\partial\mathcal{U}(x,y)}{\partial n}\right)ds(y), \tag{7}$$

where n is the unitary normal vector on the boundary and $\mathcal{U}$ is Green's function. In the 2D case, this function has this expression:

$$\mathcal{U}(x,y)=-\frac{1}{2\pi}\ln(\|x-y\|). \tag{8}$$

We express the state function on both boundaries and obtain

$$\begin{cases} u(x)=\int_{\Gamma_T}\left(-u(y)\frac{\partial\mathcal{U}}{\partial y}\right)ds+\int_{\Gamma_H}\left(\eta(y)\mathcal{U}-\tau(y)\frac{\partial\mathcal{U}}{\partial y}\right)ds, & x\in\Gamma_T,\\ \tau(x)=\int_{\Gamma_T}\left(-u(y)\frac{\partial\mathcal{U}}{\partial y}\right)ds+\int_{\Gamma_H}\left(\eta(y)\mathcal{U}-\tau(y)\frac{\partial\mathcal{U}}{\partial y}\right)ds, & x\in\Gamma_H. \end{cases} \tag{9}$$

In the classical formulation, η is formally eliminated so that u is expressed as a function of τ. Problem (5) is written as

$$t=\arg\min_{\tau}\|u-T\|_{L^2(\Gamma_T)}, \tag{10}$$

with (u,τ) satisfying (9). We introduce here a new formulation, which, on the contrary, relies on the fact that the state function u depends on both η and τ. In this generalized formulation, we keep both (η,τ) so problem (5) is written as

$$(\varphi,t)=\arg\min_{(\eta,\tau)}\|u-T\|_{L^2(\Gamma_T)}, \tag{11}$$

with (u,η,τ) satisfying (9).

4.2. The energy like error functional

In this part, the domain Ω can be 2D or 3D and the conductivity can be heterogeneous and anisotropic. The approach in the energy-like error functional method developed in Andrieux et al. [3] follows two steps. First, we consider, for a given pair (η,τ), the two following mixed well-posed problems:

$$\begin{cases} \nabla\cdot\sigma\nabla u_1=0 & \text{in } \Omega,\\ u_1=T & \text{on } \Gamma_T,\\ \sigma\nabla u_1\cdot n=\eta & \text{on } \Gamma_H, \end{cases} \tag{12}$$

$$\begin{cases} \nabla\cdot\sigma\nabla u_2=0 & \text{in } \Omega,\\ u_2=\tau & \text{on } \Gamma_H,\\ \sigma\nabla u_2\cdot n=0 & \text{on } \Gamma_T. \end{cases} \tag{13}$$

The second step is to build an energy-like error functional on the pair (η,τ) using a seminorm H^1 denoted E. Indeed, these fields are obviously equal only when the pair (η,τ) meets the real data (φ,t) on the boundary Γ_H. We propose then to solve the data completion problem via the following minimization one:

$$(\varphi,t)=\arg\min_{\eta,\tau}E(\eta,\tau), \tag{14}$$

with

$$E(\eta,\tau)=\frac{1}{2}\int_{\Omega}\sigma(\nabla u_1-\nabla u_2)^2, \tag{15}$$

with u_1 solution of (12) and u_2 solution of (13) where $\eta\in H^{-1/2}(\Gamma_H)$ and $\tau\in H^{1/2}(\Gamma_H)$.

Using Green theorem this functional can be expressed as a boundary control:

$$E(\eta,\tau)=\int_{\Gamma_T}\sigma\nabla u_1\cdot n(T-u_2)+\int_{\Gamma_H}(\eta-\sigma\nabla u_2\cdot n)(u_1-\tau). \tag{16}$$

5. Discrete formulations

In order to solve (9) or (12) and (13), we have to define a discrete formulation. When we consider a homogeneous 2D domain, the boundary element method (BEM) is well suited for solving (9). On the other hand, for the general case a finite element method (FEM) is preferable for solving (12) and (13).

5.1. The classical and generalized least-squares discrete methods

We use a boundary element method (BEM) to discretize problem (9), which can be written as

$$\begin{pmatrix} A_{11} & A_{12} & A_{13}\\ A_{21} & A_{22} & A_{23} \end{pmatrix}\begin{pmatrix} x_1\\ x_2\\ y \end{pmatrix}=0, \tag{17}$$

where x_1 is the discretization of τ, x_2 is the discretization of η and y is the discretization of T.

In the classical least-squares formulation, the unknown x_2 is eliminated by inverting A_{22} then y is computed by inverting the Schur complement matrix; the solution y can be expressed with the so-called *transfer matrix* $\mathcal{T}$, giving $y=\mathcal{T}x_1$. The discrete

classical least-squares problem is thus

$$\min_{x_1} \|\mathcal{T}x_1 - y_T\|_2, \tag{18}$$

where y_T discretize T on Γ_T, or equivalently

$$\min_{x_1} \|y - y_T\|_2 \quad \text{subject to } y = \mathcal{T}x_1. \tag{19}$$

We keep both x_1 and x_2 in the generalized least-squares problem, so we have

$$\min_{(x_1,x_2)} \|y - y_T\|_2 \quad \text{subject to} \tag{20}$$

$$\begin{pmatrix} A_{11} & A_{12} \\ A_{21} & A_{22} \end{pmatrix} \begin{pmatrix} x_1 \\ x_2 \end{pmatrix} + \begin{pmatrix} A_{13} \\ A_{23} \end{pmatrix} y = 0. \tag{21}$$

These two problems are equivalent. Now, both discrete problems must be regularized and we choose Tikhonov method in both cases. The classical regularized method is [29]

$$\min_{x_1} (\|y - y_T\|_2^2 + \lambda^2 \|x_1\|_2^2) \quad \text{subject to } y = \mathcal{T}x_1. \tag{22}$$

On the other hand, the generalized regularized method is [17]

$$\min_{(x_1,x_2)} (\|y - y_T\|_2^2 + \lambda^2 (\|x_1\|_2^2 + \|x_2\|_2^2)) \quad \text{subject to (21)}. \tag{23}$$

These two methods are no longer equivalent.

5.2. The energy like error discrete method

The implementation of the energy-like error method can be carried out using finite element method (FEM). The components of the gradient of the functional E can be computed in an efficient way by using the adjoint state method, which makes it possible to evaluate the gradient in any direction using only the determination of two adjoint fields. The derivative of the adjoint state is preferably established on the basis of the FEM discretized problem. The advantage of this fully discrete approach is that the exact gradient of the discrete objective function is obtained; moreover it is easy to implement it in existing FEM software.

We consider a mesh of Ω characterized by N nodes. The discretized forms of the problems (12) and (13) are

$$KU_1 = F_1, \tag{24}$$

$$KU_2 = F_2, \tag{25}$$

where K is the overall $N \times N$ stiffness matrix, U_1 and U_2 are the nodal variables vectors, and F_1 and F_2 are the load vectors. Vectors F_1 and U_2 can be split as follows: $F_1 = \{X_\eta, Y_F\}^T$, where X_η contains the nodal loads on Γ_H and depends explicitly on η, while Y_F gathers fluxes left unknown by the boundaries conditions of (12). The components of U_1 defined on Γ_T are fixed, the others depend implicitly on η. Likewise, U_2 can be split into two subvectors: $U_2 = \{X_\tau, Y_U\}^T$, where X_τ gathers the prescribed nodal variables associated with τ, while Y_U collects all nodal variables left unknown by the boundaries conditions of (13). The components of F_2 defined on Γ_T are prescribed, while the others are unknown and hence depend implicitly on τ. However, notice that the matrix K is constant. We rewrite (24) and (25) as

$$KU_1 = \begin{Bmatrix} X_\eta \\ Y_F \end{Bmatrix}, \tag{26}$$

$$K \begin{Bmatrix} X_\tau \\ Y_U \end{Bmatrix} = F_2, \tag{27}$$

Then, X_η and X_τ are the discretized design variables of the optimization problem described above (14). The energy-like function, in its discretized form, can be written as follows:

$$E(U_1(X_\eta), U_2(X_\tau)) = \tfrac{1}{2}(U_1^t K U_1 + U_2^t K U_2 - 2U_1^t K U_2). \tag{28}$$

To evaluate the derivatives of E we use the adjoint method. The following Lagrangian is hence defined by

$$L(U_1, U_2, \lambda_1, \lambda_2; X_\eta, X_\tau) = E(U_1, U_2, X_\tau, X_\eta) + \lambda_1^t (F_1 - KU_1) + \lambda_2^t (F_2 - KU_2), \tag{29}$$

where λ_1 and λ_2 are vectors of Lagrange multipliers, which will be used to eliminate the implicit sensitivity terms. Differentiation of (29) with respect to the design parameters yields:

$$\frac{dE}{dX_\eta} = \lambda_1^t \frac{\partial F_1}{\partial X_\eta} = \lambda_1|_{\Gamma_H}, \tag{30}$$

$$\frac{dE}{dX_\tau} = \left(\frac{\partial E}{\partial U_2} - \lambda_2^t K\right) \frac{\partial U_2}{\partial X_\tau} = K(U_2 - U_1 - \lambda_2)|_{\Gamma_H}, \tag{31}$$

where λ_1 is solution of (32) which is referred to as adjoint problem for the adjoint response λ_1 with the adjoint load $\partial E/\partial U_1$:

$$K\lambda_1 = \frac{\partial E}{\partial U_1} = K(U_1 - U_2) \quad \text{and} \quad \lambda_1 = 0 \quad \text{on } \Gamma_T \tag{32}$$

and λ_2 is solution of (33) which is referred to as adjoint problem for the adjoint response λ_2 with the adjoint load $\partial E/\partial U_2$:

$$K\lambda_2 = \frac{\partial E}{\partial U_2} = K(U_2 - U_1) \quad \text{and} \quad \lambda_2 = 0 \quad \text{on } \Gamma_H \tag{33}$$

The adjoint method requires the solution of two adjoint problems (32) and (33) for each response functional E, it is efficient when the number of functionals and constraints is small compared to the number of design parameters.

In order to optimize the computational cost, we adopt the Trust Region Method [10] to solve this optimization problem. Each iteration involves, the solution of four linear systems (24), (25), (32) and (33). More details are given on this topic in Baranger et al. [5,6], Andrieux et al. [1–4] where this method is applied to 2D and 3D linear elasticity field to identify nonlinear boundary conditions and [12,13] where it is used in hydrogeology contex.

6. Numerical trials

Computations have been run on FemLab [14] for the energy error functional and [24] for the classical and generalized least-squares methods. To test the efficiency of the proposed reconstruction processes, we resort to synthetic data obtained from the numerical solving of the forward problem (6). We test the capability of the three reconstruction methods and compare their accuracy and robustness by the mean of different experiments: in the first class of experiments, we consider a simple 2D geometry with a homogeneous conductivity ($\sigma = 1$ in Ω). In the second class of experiments, we consider a complex 2D geometry with a heterogeneous and anisotropic geometry.

For the energy like error functional, simulations are performed with finite elements of class C^1, the mesh is regular and consists of triangular elements with linear interpolation, characterized by n_n nodes and n_m elements. For both FEM and BEM we use p nodes over the heart surface and q nodes over the torso surface. We recall that there is no regularization parameter in the energy like method.

In the legends of the figures, Energy denotes the results from the energy like error functional, GLS those of the generalized least-squares method and CLS those of the classical least-squares method.

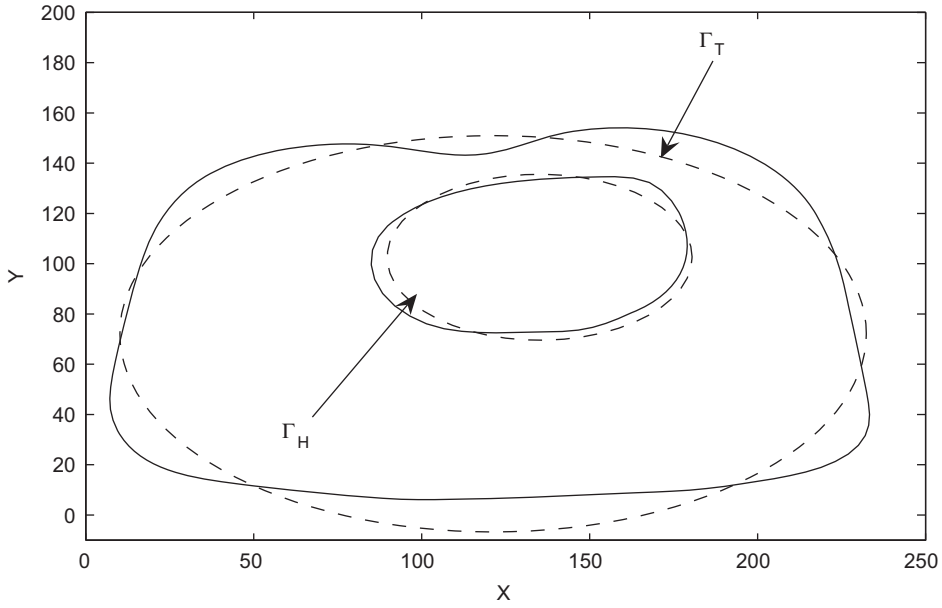

Fig. 1. The actual geometry and the approximated one (two ellipses) for the human heart and torso.

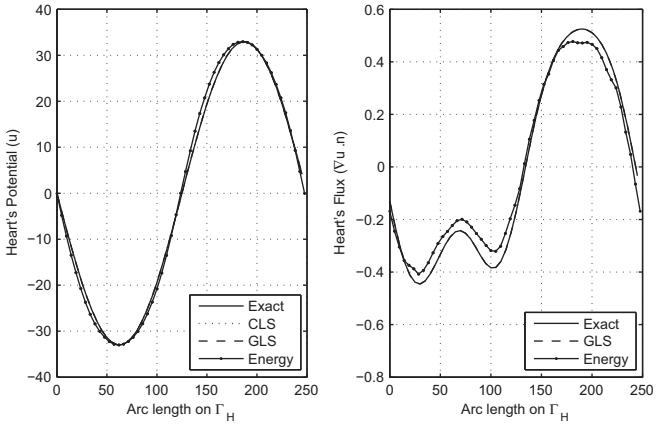

Fig. 2. Reconstructed potential and flux on the heart from a sinusoidal potential.

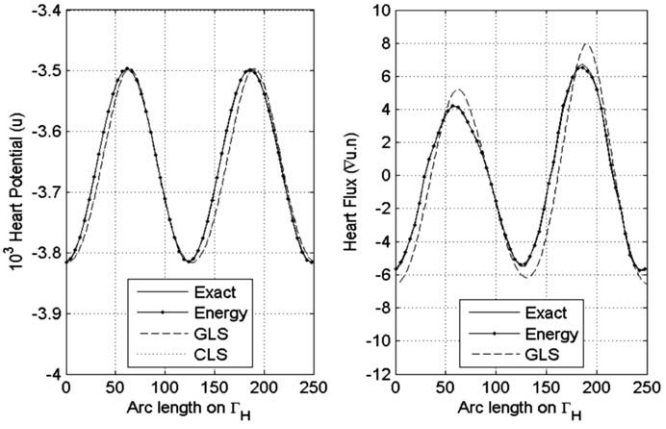

Fig. 3. Reconstructed potential and flux on the heart from overspecified data generated by $u = 10^3 \times \ln(1/(\|z-\alpha\|))$ with $\alpha = 14-30i$.

Notice that on the plot of the heart flux there is no curve corresponding to the classical least-squares method because this method does not give directly the unknown flux.

6.1. Homogeneous case without noise

The considered geometry corresponds to a transversal section of Torso-Heart which is, as illustrated in Fig. 1, well approached by two ellipses. This is in accordance with the studies done by Rudy et al. [26] in which they use a concentric and eccentric spheres for the 3D case. The selected potentials correspond to data ranging from very smooth to severely singular one.

The first numerical trial corresponds to a smooth case: the Dirichlet condition of problem (6) τ, is a sinusoidal function. Fig. 2 illustrates the obtained result. We use a mesh with n_n=544, n_m=88, p=28 and q=60.

Next experiments deal with more difficult types of potential. In all of them, we use a mesh with n_n=2057, n_m=172, p=52 and q=120.

The second series of tests is based on a *pointwise source* potential induced by $u = \ln(1/\|z-\alpha\|)$. We consider three

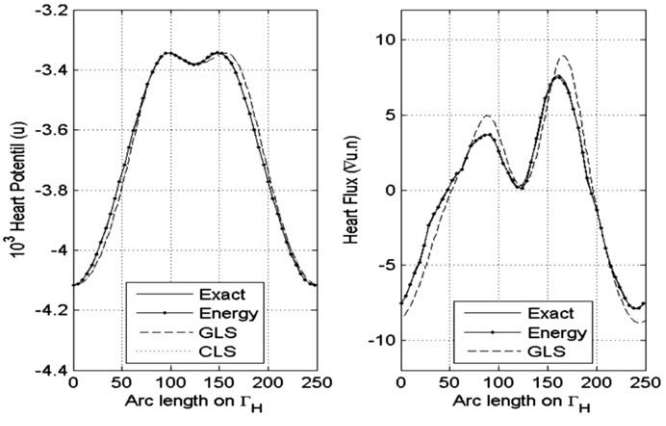

Fig. 4. Reconstructed potential and flux on the heart from overspecified data generated by $u = 10^3 \times \ln(1/(\|z-\alpha\|))$ with $\alpha = 30-30i$.

cases: the position is in the center of the heart (Fig. 3), near the heart surface (Fig. 4) and near the torso surface (Fig. 5). Note that the center of the ellipse-torso is taken as the origin of the system

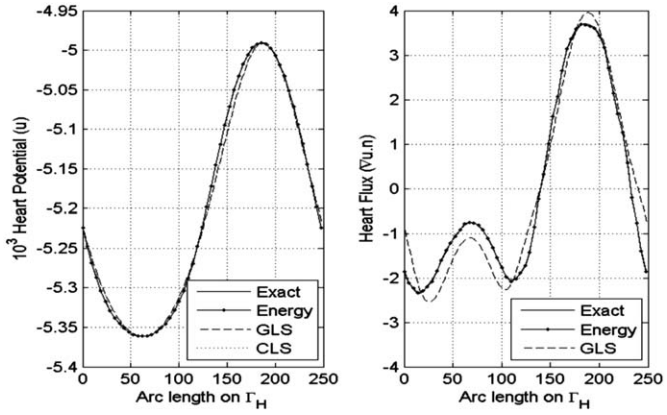

Fig. 5. Reconstructed potential and flux on the heart from overspecified data generated by $u = 10^3 \times \ln(1/(\|z-\alpha\|))$ with $\alpha = 14+150i$.

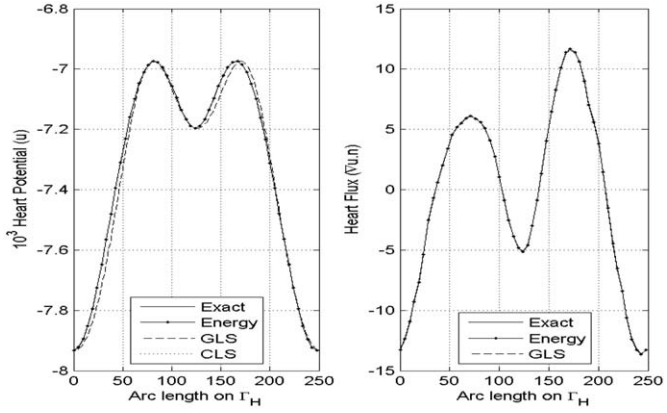

Fig. 6. Reconstructed potential and flux on the heart from overspecified data generated by $u = 10^3 \times (\ln(1/(\|z-\alpha\|)) + \ln(1/(\|z-\alpha_1\|)))$ with $\alpha = 14-30i$ and $\alpha_1 = 30-30i$.

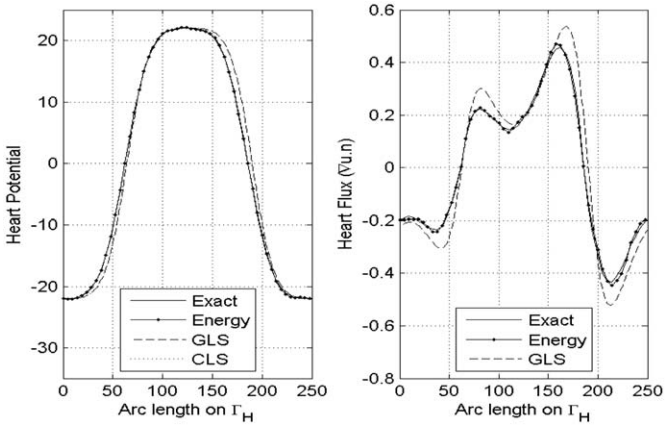

Fig. 7. Reconstructed potential and flux on the heart from overspecified data generated by $u = 10^3 \times Re(1/(z-\alpha)$ with $\alpha = 14-30i$, so the singular data is in the center of the heart ellipse.

coordinates. Fig. 6 illustrates the results for *multiple pointwise* potential.

The third series of tests is induced by *singular* data associated to $u = Re(1/(z-\alpha))$, where $z=x+iy$, is the affix of the current point $M(x,y)$ and $\alpha = a+ib$. We consider three cases: the singular data

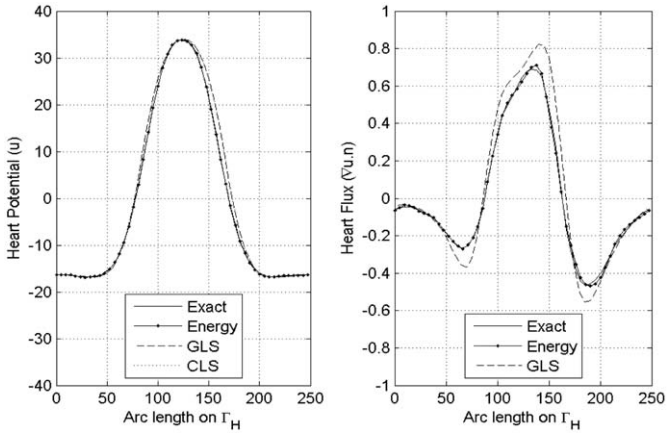

Fig. 8. Reconstructed potential and flux on the heart from overspecified data generated by $u = 10^3 \times Re(1/(z-\alpha))$ with $\alpha = 30-30i$, so the singular data are near the heart ellipse.

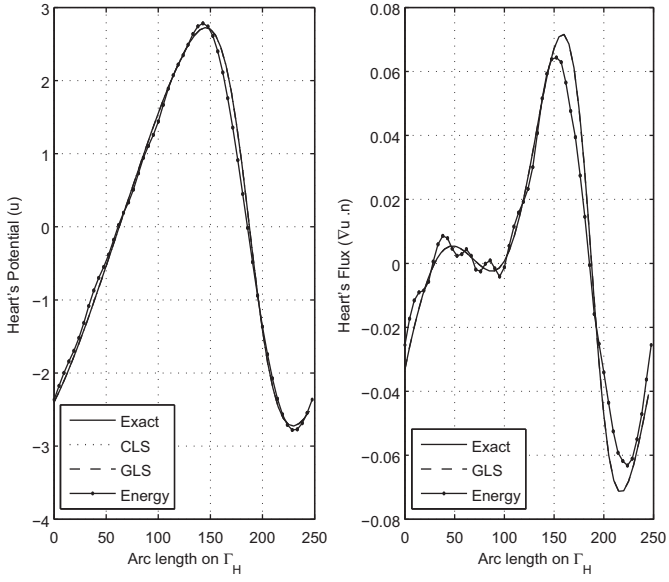

Fig. 9. Reconstructed potential and flux on the heart from overspecified data generated by $u = 10^3 \times Re(1/(z-\alpha))$ with $\alpha = 14+150i$, so the singular data are near the torso's ellipse.

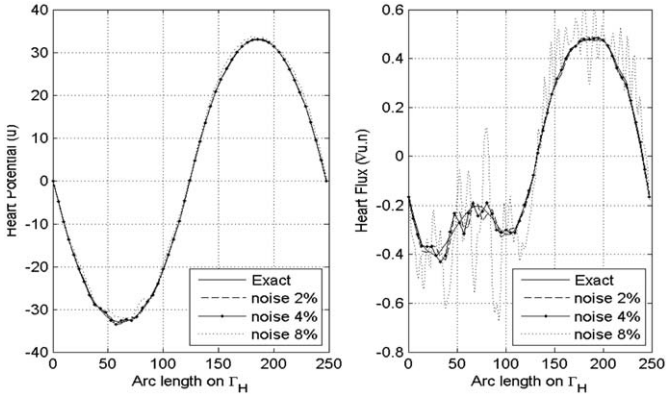

Fig. 10. Reconstructed potential and flux on the heart from a sinusoidal potential with different levels of noise.

are in the center of the heart ellipse (Fig. 7), in the vicinity of the heart (Fig. 8) and in the vicinity of the torso (Fig. 9).

For all these examples the three considered recovering processes (CLS, GLS and Energy) lead to a very satisfactory reconstruction of the potential. The classical method CLS does not recover directly the flux on the heart, while both methods GLS and Energy give a correct estimation of the flux. However, as expected, better reconstruction is obtained by the two proposed methods when we deal with smooth data. Slight degradation is observed when one deals with singular fields.

Table 2
Various noise levels, in the case of a singular data generated by $u = 10^3 \times Re(1/(z-\alpha))$ with $\alpha = 14-30i$.

Noise level (%)	1	2	3	4	5	8
E (Energy) (%)	2.52	2.71	3.52	6.59	9.31	10.02
E (GLS) (%)	2.56	5.18	5.75	7.10	9.14	12.37

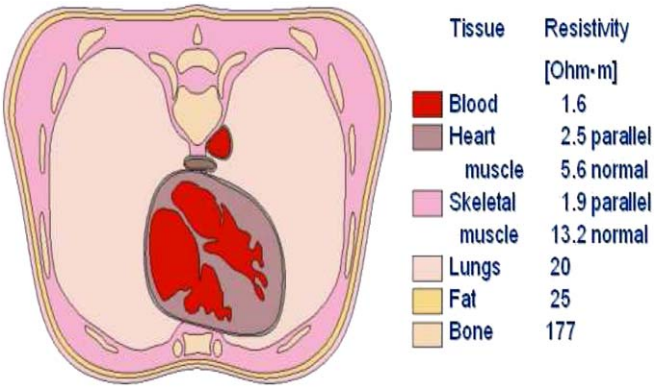

Fig. 11. A real geometry of a human torso with the different resistivities [23].

6.2. Homogeneous case with noise

We now analyze the sensitivity of the two reconstruction methods, Energy and GLS, with respect to noisy data. We still consider the same geometry with $\sigma = 1$. A noise with null mean is applied to the measurements on the torso. In Fig. 10 we show the reconstructed heart potential and flux for different levels of noise in the case of smooth data. We observe that the heart potential is well identified, however, the heart flux deteriorates when the level of the noise is greater than 8%.

We define the relative error as

$$E = \frac{\|u_{exact} - u_{compute}\|_{L^1}}{\|u_{exact}\|_{L^1}} * 100, \tag{34}$$

where u is the heart potential. We compare the two methods in the case of a singular data. Table 2 shows the relative error with different levels of noise up to 8%.

6.3. Heterogeneous anisotropic case

In this general case, we consider only the FEM method. To go through more realistic case, we test our energy-like error functional with the model described in Fig. 11. Let us first recall that the electric source lies within the heart, whereas the volume conductor contains the heart and the remaining organs in the torso. We consider an electro-physiological model where the various electrical resistivities are given for lungs, surface muscle, fat and bones are considered [23]. This model takes into account the heterogeneity as well as the anisotropy of the volume conductor. We use a slightly simplified model which is illustrated in Fig. 12. We consider a singular case with $u = Re(1/(z-\alpha))$ with $\alpha = 7-6i$. Our results without noise show that the reconstructed data are in good agreement with the actual ones (see Fig. 13). We also consider the same case with noise until 10% and, as shown in Fig. 14, results are very satisfactory.

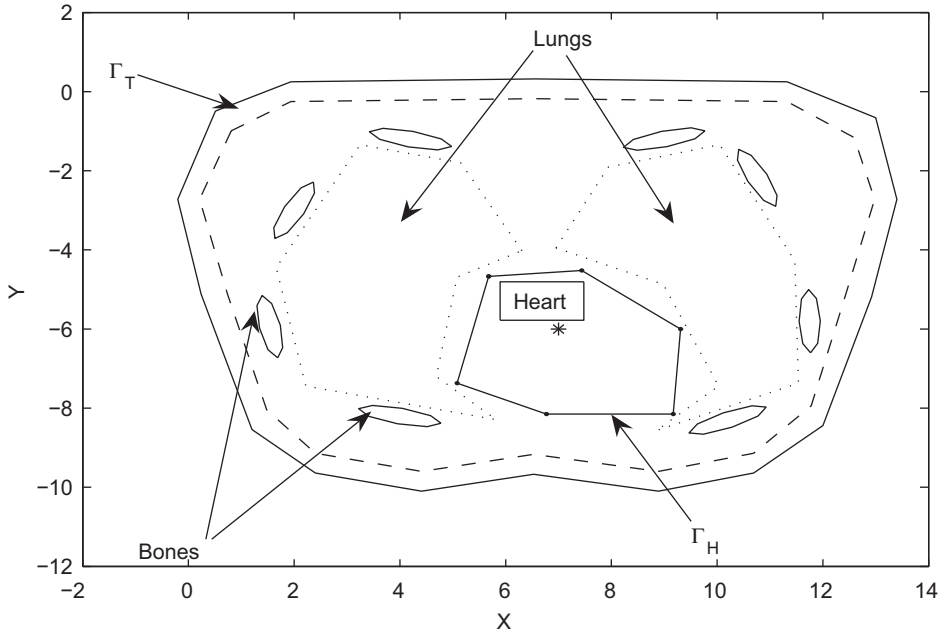

Fig. 12. Modelized heterogeneous and anisotropic geometry for study.

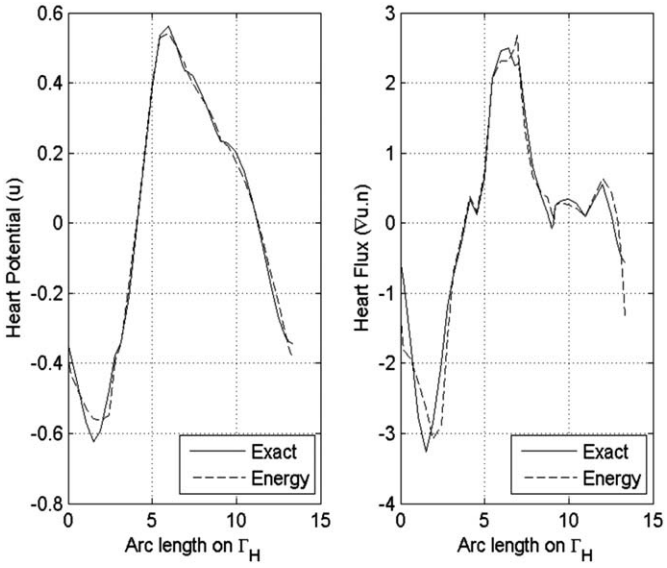

Fig. 13. Reconstructed potential and flux on the heterogeneous heart from overspecified data generated by $u = Re(1/(z-\alpha))$ near the heart.

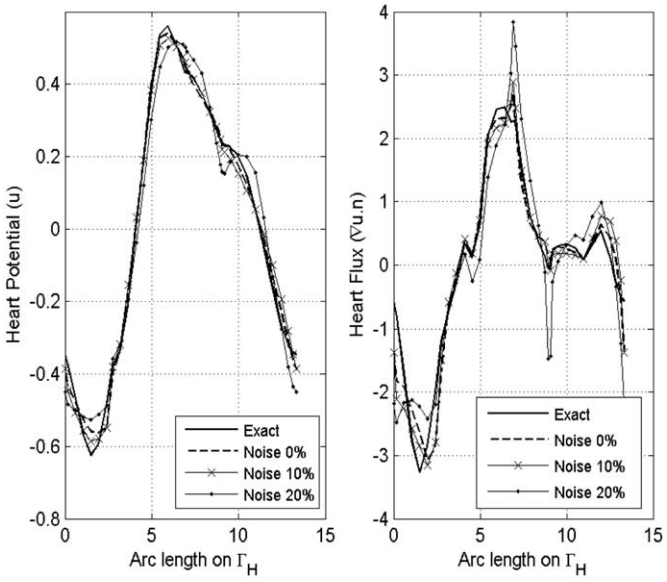

Fig. 14. Reconstructed potential and flux on the heterogeneous heart from overspecified data generated by $u = Re(1/(z-\alpha))$ near the heart with different level of noise.

7. Conclusion

In this work, we design a minimization of an energy error functional (Energy) and a generalized least-squares method (GLS) for recovering the cardiac electrical properties from the body-surface electrical activity (current flux and potential). The peculiar character of the two methods lies on the treatment of the reconstructed potential and current flux: in contrast to the classical least-squares method (CLS), the cardiac potential and the flux are both recovered.

We run numerical experiments in the 2D case. For a homogeneous domain, the boundary element method is easy to implement and cheaper than the finite element method. Our two methods (Energy and GLS) recover correctly the potential and the flux, also in the presence of noise. Thus the regularized GLS approach should be preferred, because of low computational requirements.

However, for a heterogeneous anisotropic domain, it is not easy at all to use the boundary element method, whereas the finite element method is efficient. Thus the Energy method is relevant here. As highlighted by the numerical experiments, the Energy method recovers potential and flux, also with noise.

It should be noted that the Energy method does not require any regularization parameter. It is a general recovering process for data completion problems. As shown in [1,6,5,12,13], this method can be easily implemented to deal with different physical models (fluid or solid mechanics), nonlinear and time dependent problems.

Acknowledgments

N. Hariga's work is supported by the Ministère de la Recherche Scientifique, de la Technologie et du Développement des Compétences (MRSTDC, Tunisia) under the *LAB-STI-02 Program* and partially by the associated team INRIA/LAMSIN *Enee* and *SARIMA* project through SARIMA-TAMTAM. T. Baranger work is supported by Aire-développement within the program *Equipe référence AIRE développement* (*IRD*). J. Erhel work is partly supported by *STIC 05I16* INRIA-DGRST.

References

[1] Andrieux S, Baranger TN. Energy error based numerical algorithms for Cauchy problems for nonlinear elliptic or time dependent operators. In: 2009 inverse problems symposium, Michigan State University, 30 May–2 June 2009.
[2] Andrieux S, Baranger TN. An energy error-based method for the resolution of the Cauchy problem in 3D linear elasticity. Comput Meth Appl Mech Eng 2008;197(9–12):902–20.
[3] Andrieux S, Baranger TN, Ben Abda A. Solving Cauchy problems by minimizing an energy-like functional. Inverse Problems 2006;22:115–33.
[4] Andrieux S, Baranger TN. Energy method for Cauchy problems of evolutions equations. In: 6th international conference on inverse problems in engineering: theory and practice Dourdan (Paris), France—June 15–19, 2008.
[5] Baranger TN, Andrieux S. An optimization approach for the Cauchy problem in linear elasticity. J Multidisciplinary optim 2008;35:141–52.
[6] Baranger TN, Andrieux S. Energy methods for boundary conditions identification for dynamic problems. In: 8th world congress on computational mechanics (WCCM8) and the 5th European congress on computational methods in applied sciences and engineering (ECCOMAS 2008), Lido Island in Venice (Italy) on 30 June–4 July 2008, 2008.
[7] Chakib A, Nachaoui A. Convergence analysis for finite approximation to an inverse Cauchy problem. Inverse Problems 2006;22:1191–206.
[9] Cimetière A, Delvare F, Jaoua M, Pons F. Solution of the Cauchy problem using iterated Tikhonov regularization. Inverse Problems 2001;17:553–70.
[10] Coleman TF, Li Y. An interior trust region approach for nonlinear minimization subject to bounds. SIAM J Optim 1996;6:418–45.
[11] Erhel J, Canot É. The inverse electrocardiography problem viewed as a general linear model slides. In: ICIAM'03, Sydney, July 2003.
[12] Escriva X, Baranger TN, Hariga Tlatli N. Leak identification in porous media by solving the Cauchy problem. C R Mécanique 2007;335:406–10.
[13] Escriva X, Baranger TN. A variational approach to solve Cauchy problem for steady state stokes flow. In: 8th world congress on computational mechanics (WCCM8) and the 5th European congress on computational methods in applied sciences and engineering (ECCOMAS 2008), Lido Island in Venice (Italy) on 30 June–4 July 2008, 2008.
[14] FemLab. Multiphysics Modeling Copyright 1994–2004 Comsol.
[15] Gulrajani RM. The forward and inverse problems of electrocardiography. IEEE Eng Med Biol 1998;17:84–101.
[16] Hadamard J. Lectures on Cauchy's problem in linear partial differential. New York: Dover; 1953.
[17] Hansen PC. Rank-deficient and discrete Ill-posed problems, numerical aspects of linear inversion. Philadelphia: SIAM; 1998; pp. 247.
[18] Hechme G. Résolution d'un problème inverse en électrocardiographie, master thesis report, Université libanaise, AUF Beirut and INRIA Rennes, 2002; pp. 51.
[19] Huiskamp GJ, Van Oosterom A. The depolarization sequence of the human heart surface computed from measured body surface potentials. IEEE Trans Biomed Eng 1989;35:1047–59.

[20] Hunter PJ. Bioengineering notes, 2000.
[21] Khoury DS, Taccardi B, Lux RL, Ershler PR, Rudy Y. Reconstruction of endocardial potentials and activation sequences from intracavity probe measurements. Circulation 1995;91:845–63.
[22] MacLeod RS, Brooks DH. Recent Progress in inverse problems of electrocardiography. IEEE Eng Med Biol 1998;17:23–83.
[23] Malmivuo Jaakko 〈http://butler.cc.tut.fi/~malmivuo/bem/index.htm〉.
[24] Matlab Sofware Copyright The MathWorks, Inc, 1984–2000.
[25] Messnarz B, Tilg B, Fischer G, Hanser F. A new spatiotemporal regularization approach for reconstruction of cardiac transmembrane potential patterns. IEEE Trans Biomed Eng 2004;51:273–81.
[26] Rudy Y, Plonsey R. The eccentric spheres model as the basis for a study of the role of geometry and inhomogeneities in electrocardiography. IEEE Trans Biomed Eng 1979;26:392–9.
[29] Tikhonov AN, Arsenin VY. Solution to Ill-posed problems. New York: Winston-Wiley; 1977.